

Original Article

Optimization of Machining Parameters of Al6061/SICMMCs Using Taguchi Approach

Ajit Katkar¹, Bharat Sudame², Smita Nande³, Ravindra Joshi⁴, Amit Kasar⁵, Amruta Patil⁶

¹Department of Mechanical, Sanjeevan College of Engineering, Panhala, Maharashtra, India.

²Department of Electrical, Yashvantrao Chavan College of Engineering, Nagpur, Maharashtra, India.

^{3,4,5}Department of Engineering Sciences, International Institute of Information Technology, Pune, Maharashtra, India.

⁶Department of Computer, Vishwakarma Institute of Technology, Pune, Maharashtra, India.

⁵Corresponding Author : amit.kasar1982@gmail.com

Received: 08 September 2025

Revised: 09 October 2025

Accepted: 10 November 2025

Published: 28 November 2025

Abstract - Aluminum alloys are extensively used in transportation and process industries because they offer low mass, good thermal conductivity, and ease of fabrication. To support reliable machining of aluminum matrix composites for such applications, this work examines the turning performance of SiC-reinforced Al6061 composites and determines optimal cutting conditions to balance quality and productivity. Al6061/SiC composites were produced by gravity die casting with reinforcement levels of 2–8 wt%. Optical microscopy and SEM/EDS confirmed a uniform dispersion of SiC particulates, clean particle–matrix interfaces, and the absence of detectable reaction products or porosity at the examined scales. Machining experiments were structured using a Taguchi L16 orthogonal array to study the influence of cutting speed (180–500 rpm), feed rate (0.1 mm/rev), depth of cut (0.3–1.2 mm), and SiC fraction on key outcomes: Surface Roughness (R_a), Material Removal Rate (MRR), and Tangential Force (F_t). Signal-to-noise analyses used larger-is-better for MRR and smaller-is-better for R_a and F_t , while ANOVA quantified factor significance. Results show that cutting speed is the primary driver for MRR, SiC content has the most potent effect on R_a , and depth of cut most strongly influences F_t . ANOVA corroborated these rankings, identifying cutting speed, SiC fraction, and depth of cut as the dominant contributors to variability in MRR, R_a , and F_t , respectively. The study provides practical parameter windows for turning Al6061/SiC composites, demonstrating that appropriate selection of speed, feed, and DOC can deliver smooth surfaces and competitive throughput despite the increased abrasiveness at higher SiC contents.

Keywords - Analysis of Variance (ANOVA), Cutting speed, Material Removal Rate (MRR), Surface Roughness (R_a), Taguchi Method.

1. Introduction

The rapid adoption of lightweight, high-performance materials has revolutionized contemporary machining practices. Among these, Aluminium Metal Matrix Composites (Al-MMCs) reinforced with ceramic particulates have drawn particular interest because they deliver high specific strength, dimensional stability, and improved thermal performance. Their relevance spans automotive, aerospace, and defense applications where components must combine low mass with high durability and wear resistance.

Aluminium alloys are attractive matrices thanks to their low density, favourable strength-to-weight ratio, corrosion resistance, and manufacturability. Yet near-net-shape routes rarely eliminate the need for finish machining, especially when tight tolerances and stringent surface integrity are required. The introduction of hard reinforcements such as SiC, Al₂O₃, or TiC makes these materials intrinsically anisotropic and abrasive, altering chip formation and tool–work interactions compared with monolithic aluminium. As

a result, selecting cutting parameters becomes non-trivial: a soft, ductile matrix coexists with hard, angular particles that promote micro-fracture, ploughing, and localized heat generation. Processing history—specifically, heat treatment conditions, particle size, and the uniformity of reinforcement distribution—further modulates machinability [1-4].

Parameter sets that work well for unreinforced alloys often fail in Al-MMCs, manifesting as accelerated tool wear, elevated cutting forces, and deteriorated surface finish. Because many reinforcements exceed the hardness of HSS and standard carbides, flank and crater wear can progress rapidly, particularly in precipitation-strengthened 6xxx alloys such as Al6061 that already contain challenging intermetallic phases.

A clear understanding of chip morphology, shear localization, and force evolution during turning is therefore essential to improve both surface quality and process economics [5-8, 11].



Design-of-experiments approaches, especially Taguchi methods, have been widely used to identify influential factors such as cutting speed, feed, depth of cut, and reinforcement fraction. Prior studies on systems such as Al2024/Al2O3 and various hybrid composites containing fly ash or graphite often report feed and speed as the dominant factors for surface roughness, with ANOVA employed to rank the effects. However, findings from hybrids with solid lubricants or from different matrices do not directly transfer to binary Al6061/SiC, where frictional and thermal behaviors differ, and tool degradation mechanisms can be more severe [12, 16, 17].

Using a Taguchi experimental design, the authors adjusted cutting parameters for machining squeeze-cast Al6061–SiC MMCs. Cutting speed and feed emerged as the primary drivers of tool wear, demonstrating Taguchi's effectiveness in reducing wear and improving machining efficiency.

Applying the Taguchi approach to Al6061 composite wear tests, the study found that SiC content and applied load most strongly governed wear rate and friction, indicating clear levers for enhancing durability [19].

For stir-cast Al6061–SiC–fly ash composites, the inclusion of fly ash improved wear resistance while lowering density, supporting lightweight and more sustainable material design [20].

Under dry sliding, Al6061 reinforced with a hybrid of SiC and B4C nano particles showed higher hardness and better wear resistance than composites reinforced with SiC alone.

Temperature effects and sustainability aspects, such as dry versus MQL environments.

2. Research Gap and Problem Statement

Despite extensive work on Al-MMCs, a focused Taguchi-only optimization for binary Al6061/SiC turning remains limited. Typical limitations in the literature include:

Consequently, there is an outstanding need to clarify, for the pure Al6061/SiC system:

- The individual and combined effects of feed, cutting speed, depth of cut, and SiC content on surface roughness and tool wear in turning.
- The thermo-mechanical response of the composite under varying parameter sets.
- The role of sustainable lubrication strategies (dry/MQL) in improving machinability and tool life.

Objectives of the present work

- Apply a Taguchi design with ANOVA to optimize

turning parameters for Al6061/SiC composites.

- Investigate the effects of feed (0.1–0.4 mm/rev), cutting speed (180–500 rpm), depth of cut (0.3–1 mm), and SiC reinforcement (2–6 wt%) on key responses.

Identify the most influential factors and practical parameter windows for:

- Minimizing surface roughness,
- Maximizing material removal rate (MRR), and
- Reducing tangential cutting force.
- Formulate a machining strategy that balances surface quality, productivity, and tool life for binary Al6061/SiC composites, with considerations for sustainable operation
- Emphasis on hybrid systems (e.g., Al/SiC/graphite), where graphite alters friction, heat dissipation, and wear mechanisms.
- Reliance on multi-criteria or hybrid optimizers (e.g., Taguchi combined with grey relational or other techniques), obscuring direct factor–response relationships obtainable from Taguchi alone [9, 10].
- Narrow response scopes centered on surface roughness, with limited attention to tool wear progression, cutting

3. Existing Studies Based on Taguchi's Approach

In 2025, Taguchi-style design of experiments continued to be the go-to, budget-friendly framework for tuning machining and tribological performance of Al6061–SiC and related hybrid MMCs. A consistent workflow has crystallized: use Taguchi orthogonal arrays for factor screening and main-effect estimation, apply ANOVA to quantify contribution and significance, and add an MCDM layer—TOPSIS, Entropy–CoCoSo, or Grey Relational Analysis—to balance multiple objectives such as surface finish, MRR, tool wear, burr control, and surface integrity [18, 21, 22].

Manickam and colleagues utilized Taguchi S/N statistics in conjunction with TOPSIS to rank drilling parameters for Al6061/Al6063–SiC–ZrO2 composites, subsequently verifying the composite index through confirmation runs and microscopy, which demonstrated improved hole quality without compromising the microstructure [21]. Basar et al. combined a Taguchi array with Entropy weighting and the CoCoSo decision model to co-optimize six drilling quality indicators in hot-pressed Al/B4C/SiC hybrids, delivering both the best operating window and a sensitivity map linking reinforcement fraction to drilling outcomes [22]. Sathiyaraj's work used Taguchi L-series arrays with ANOVA for pin-on-disc wear of Al6061–SiC, showing that within the optimized window, higher SiC content improved wear resistance, while load and sliding speed dominated the response [18].

Conference and preprint results from 2025 echo these findings across drill types and SiC levels: spindle speed, feed rate, and reinforcement fraction consistently emerge as the

primary levers and are easily prioritized via Taguchi screening [23, 24]. The prevailing recommendation is to deploy Taguchi for rapid factor reduction, pair it with MCDM for multi-response ranking, and then refine the reduced set using RSM or multi-objective methods (e.g., NSGA-II) to capture interactions and nonlinear trade-offs not addressed by orthogonal arrays [18, 21-24].

4. Experimentation

4.1. Material Selection

AA6061 was used as the matrix for the Al6061/SiC metal matrix composites due to its low density, corrosion resistance, favourable strength-to-weight ratio, and castability. The reinforcement was angular Silicon Carbide (SiC) particulate with an average size of about 75 μ m, chosen to enhance hardness, thermal stability, and wear resistance. The matrix chemistry determined by wet chemical analysis was consistent with AA6061 specifications.

4.2. Fabrication of Al6061/SiC Composites

Composites were produced by mechanical-stir (vortex) casting, selected for its simplicity, low cost, and capability to disperse particulates uniformly. AA6061 ingots were melted in a graphite crucible at approximately 720°C in an electric resistance furnace. Melt degassing was performed with

hexachloroethane (C₂Cl₆) [13-15] tablets to reduce dissolved hydrogen and minimize porosity.

SiC particles were preheated at 450°C for 1 hour to remove moisture and improve wetting, then gradually fed into the melt under continuous mechanical stirring. Stirring parameters (speed and duration) were established through preliminary trials to promote homogeneous dispersion and suppress agglomeration. The composite melt was poured into preheated metal dies to obtain cylindrical blanks suitable for turning. Three reinforcement levels were prepared: 2, 4, and 6 wt% SiC. After solidification, specimens were machined to size for microstructural evaluation and machining tests.

4.3. Microstructural Characterization

Sections were prepared for metallography in accordance with ASTM E3. Samples were etched with an aluminum alloy etchant comprising 95 mL distilled water, 4 mL H₂SO₄, 4 mL HF, and 2 g CrO₃ to reveal the matrix and particle interfaces. Optical images were recorded using an Olympus metallurgical microscope. SEM (JEOL JSM-840A) was used to assess particle morphology, distribution, and matrix–particle bonding. The observations indicated a uniform dispersion of SiC, clean interfaces, and minimal porosity at the examined scales.

Table 1. Chemical composition of AA6061

Elements	Si	Ti	Fe	Mn	Zn	Cu	Mg	Cr	Other	Al
Wt. (%)	0.41-0.8	0.151	0.71	0.151	0.251	0.401	0.81-1.2	0.351	0.05	Balance

4.4. Experimental Design and Machining Parameters

The machining study employed a Taguchi design to evaluate the influence of process parameters on:

- Surface roughness (Ra)
- Material removal rate (MRR)
- Tangential cutting force (Ft)

An L16 orthogonal array was selected to explore four factors efficiently:

- A: SiC content = 2, 4, 6 wt%
- B: Cutting speed = 180–500 rpm
- C: Feed rate = 0.1–0.4 mm/rev
- D: Depth of cut (DOC) = 0.3–1.0 mm

Measurements and analysis:

- Ra measured using a stylus profilometer
- MRR computed from mass loss/volume removed and machining time
- Ft captured using a dynamometer during turning

Signal-to-noise (S/N) criteria:

- Smaller-is-better: Ra, Ft
- Larger-is-better: MRR

Through confirmation tests to assess predictive reliability.

4.5. Summary of Experimental Setup

Dry turning was carried out on a conventional engine lathe using uncoated K10-grade carbide tools. Workpieces were rigidly fixtured to maintain dimensional stability. Each experimental condition was replicated three times; average values of Ra, MRR, and Ft were used for analysis. The combined Taguchi and ANOVA framework, together with replication and confirmation trials, provides a robust basis for determining optimized machining parameters for Al6061/SiC composites.

ANOVA at a 95% confidence level quantified factor significance and contributions to response variance. Optimal settings identified from Taguchi/S/N were verified.

5. Results and Discussion

This section details the microstructural features of the produced Al6061/SiC composites and the outcomes of machining experiments, including Taguchi optimization, ANOVA-based factor significance, and chip/surface morphology from SEM observations.

5.1. SEM/EDS Characterization of SiC Particles

The as-received SiC particulates were characterized by SEM and EDS. Figure 1(a) shows that the particles possess

sharp, faceted, and irregular geometries that promote mechanical interlocking with the ductile aluminum matrix during processing. The accompanying EDS spectrum (Figure

1(b)) displays dominant peaks for silicon and carbon, confirming the expected SiC chemistry with no notable impurity peaks.

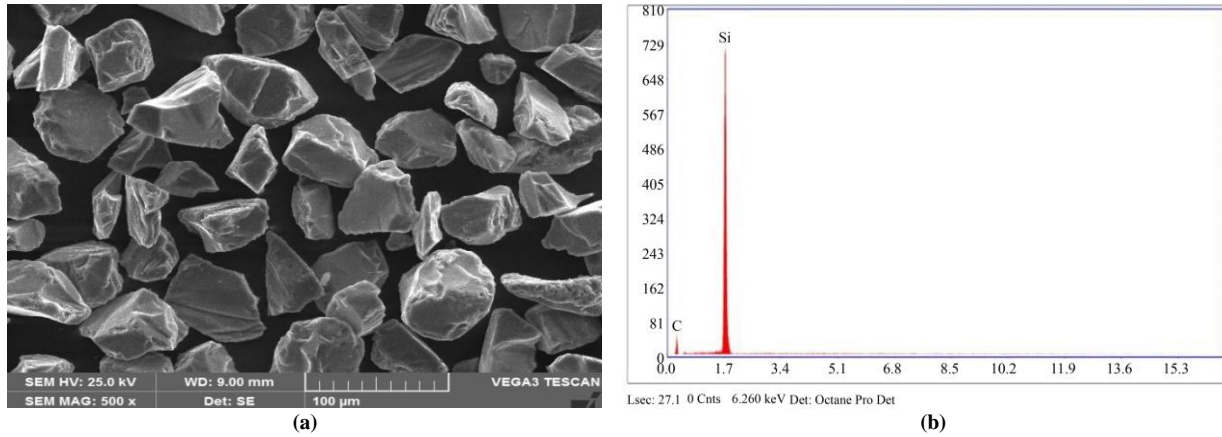


Fig. 1 (a) SEM image, and (b) EDS of SiC particles.

5.2. Microstructure of Al6061/SiC Composites

Representative optical micrographs of the cast Al6061/SiC composites are provided in Figure 2. The reinforcement appears well dispersed throughout the matrix with minimal clustering or agglomeration. Interfaces between SiC and the aluminum matrix are clean, indicating effective wetting during stir casting. No obvious porosity or reaction rims were observed at the resolution of optical microscopy,

suggesting that the applied melt treatment and degassing protocol yielded a sound microstructure.

Such a uniform spatial distribution and strong interfacial contact are expected to enhance mechanical response and wear resistance, while also contributing to consistent machinability across the bulk.

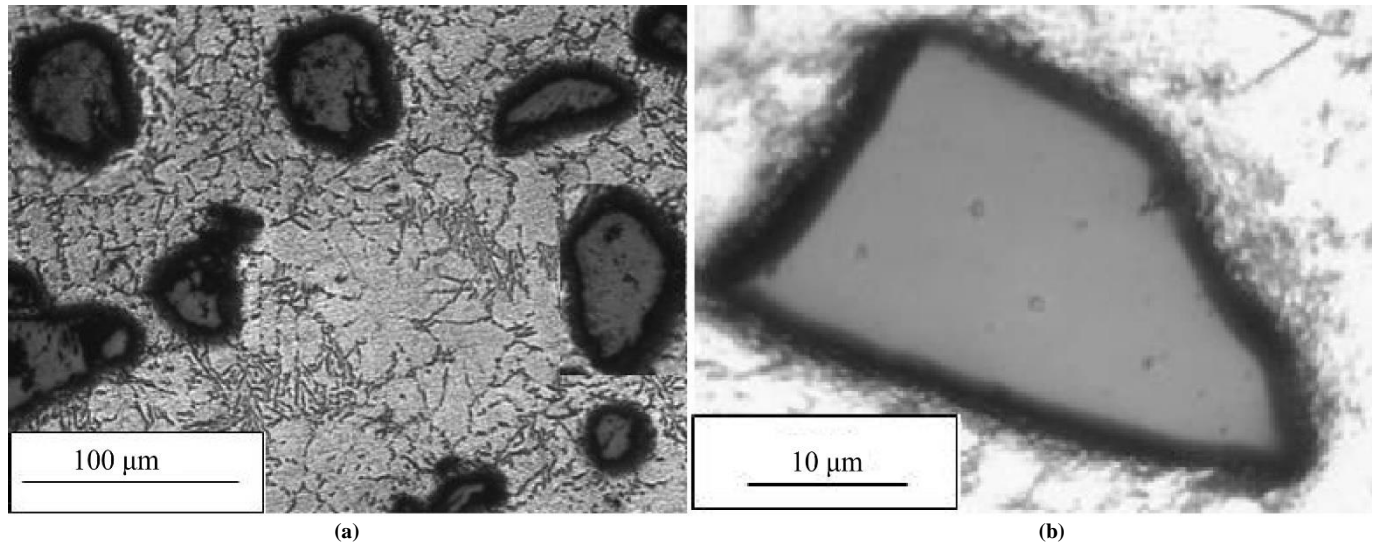


Fig. 2. Optical micrograph of Al6061/2 wt% SiC composite showing homogeneous particle distribution

5.3. SEM/EDS Confirmation of Reinforcement in the Composite

Further verification on the Al6061/2 wt% SiC material was performed via SEM/EDS (Figure 3). The SEM image (Figure 3(a)) reveals SiC particles firmly embedded within the matrix without signs of interfacial gaps or particle

pull-out. The EDS spectrum (Figure 3(b)) identifies pronounced Si and C peaks, corroborating the presence of SiC and confirming successful incorporation during casting. The observed interfacial integrity is advantageous for reliable cutting behavior, reducing the likelihood of particle dislodgement and associated surface damage during turning.

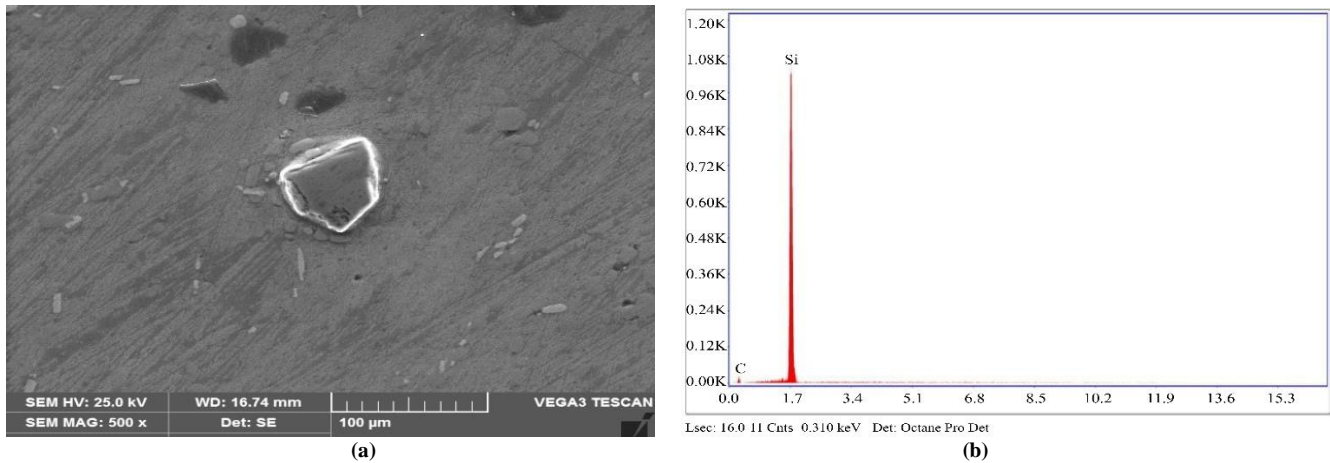


Fig. 3 (a) SEM image, and (b) EDS spectrum for Al6061/2 wt% SiC composite.

5.4. Optimization of Machining Parameters using Taguchi Design

A Taguchi L16 orthogonal array was used to study four factors—SiC content, cutting speed, feed rate, and Depth of Cut (DOC)—with the goals of minimizing Surface Roughness (Ra) and Tangential Cutting Force (Ft) while maximizing Material Removal Rate (MRR). Analyses were conducted in MINITAB (v19), and Signal-to-Noise (S/N) ratios were computed using:- Larger-is-better for MRR, - Smaller-is-better for Ra and Ft.

Mean S/N plots indicated the following:

- Surface Roughness (Ra): Lower Ra at higher cutting speeds and lower feeds, indicating smoother finishes under faster, lighter-feed conditions.
- Material Removal Rate (MRR): MRR increases notably with higher cutting speed and larger DOC, highlighting their dominant role in productivity.
- Tangential force (Ft): Ft rises with increasing feed and higher SiC fraction, reflecting the greater cutting resistance of the harder, more abrasive composite.

Table 2. Design of experiments as per L16 orthogonal array

EXPT. No.	Speed rpm	Feed mm/rev	DoC mm	% SiC	SR (μm)	SR-SNRA1	MRR	MRR-SNRA1	TF	TF-SNRA1
1	180	0.1	0.3	0	1.12	-0.9844	8343	78.4264	34	-30.6296
2	180	0.2	0.6	2	1.76	-4.9103	8489	78.5771	64	-36.1236
3	180	0.4	0.9	4	2.59	-8.266	8678	78.7684	102	-40.172
4	180	0.6	1.2	6	3.44	-10.7312	8845	78.934	144	-43.1672
5	280	0.1	0.6	4	1.76	-4.9103	8777	78.8669	71	-37.0252
6	280	0.2	0.3	6	1.92	-5.666	8956	79.0423	85	-38.5884
7	280	0.4	1.2	0	1.86	-5.3903	8942	79.0287	139	-42.8603
8	280	0.6	0.9	2	1.56	-3.8625	9023	79.107	124	-41.8684
9	450	0.1	0.9	6	1.93	-5.7111	9145	79.2237	113	-41.0616
10	450	0.2	1.2	4	2.78	-8.8809	9278	79.3491	148	-43.4052
11	450	0.4	0.3	2	2.76	-8.8182	9143	79.2218	101	-40.0864
12	450	0.6	0.6	0	2.34	-7.3843	9187	79.2635	115	-41.214
13	500	0.1	1.2	2	2.65	-8.4649	9568	79.6164	158	-43.9731
14	500	0.2	0.9	0	1.56	-3.8625	9657	79.6968	130	-42.2789
15	500	0.4	0.6	6	2.69	-8.595	9756	79.7854	169	-44.5577
16	500	0.6	0.3	4	3.3	-10.3703	9645	79.686	120	-41.5836

Speed is in rpm, Feed is in mm/rev, DOC is in mm, SR is in Microns.

5.4.1. Signal-to-Noise Ratio

The signal-to-noise was attained from the Taguchi fashion, and the impact of machining parameters like DOC and feed rate was studied. Cutting speed, and Sic Content. Parameters such as material junking rate, tangential force, and face roughness were analyzed. As mentioned preliminarily, the larger is better criterion for material removal, while the lower is better criterion for surface roughness in tangential. Forces were espoused for this present study. The ranking of machining parameters is grounded upon signal-to-noise rates tabulated in Tables 3, 4, and 5. To start with, Table 3, it can be observed that the slice speed has the loftiest influence on the material junking rate, and by feed rate, the Sic content. From Table 4, it can be observed that the Sic has the loftiest impact on the face roughness, feed rate, and DOC. Eventually, as shown in Table 5, it can be observed that the DOC exhibits the loftiest impact on tangential force, cutting speed, and feed rate. After analysing these compliances, it is relatively clear that for different responses, the dominating machining parameters are different.

The table shows the major goods plot for the signal-to-noise rate for the material junking rate for different machining parameters. It can be seen from the figure that the optimal input parameter for carrying advanced material junking rate is cutting speed with 500 rpm, the feed rate of .6 mm/ rev, DOC of 1.2 mm, and Sic content of 6 0/c. With an increase in cutting speed, the material removal rate increases linearly and

is set up to be advanced at the highest slice speed. Figure 5 shows the major goods plot for the signal-to-noise ratio for the roughness for different machining parameters. It can be seen from the figure that optimal input parameters for carrying lower face roughness are cutting speed of 280 rpm, feed rate of .1 mm/ rev, and DOC of 1.2 mm and Sic content of 4 0/ c. At these optimal machining parameters, the face roughness finish attained is good and lower for A16061/ Sic. One can see that as the feed rate increases, the face roughness increases, which is due to the fact that an increase in feed rate has caused an increase in the distance between the tool paths. Figure 6 depicts the main goods plot of the S/N rate for tangential force for different machining parameters. It can be seen from the figure that optimal input parameters for carrying lower face roughness are cutting speed with 180mm and feed rate of 0.1mm/rev, DOC to 3 mm, Sic content of 0 %. An increase in feed rate causes further material to be removed, which in turn leads to the formation of a lesser number of erected-up edges. Confirmation of a similar structure. The up edges cause difficulty in the machining, leading to an increase in the tangential slice force. Also, with the advanced Si content, the hardness of A16061 amalgamation is increased, which also increases the tangential slice force. Eventually, at advanced DOC, the contact point of flute length of the tool is increased significantly, leading to tool drooling, which in turn causes an increase in tangential slice force.

Table 3. S/N ratio response table for the Material Removal Rate

Level	Speed	Feed	DoC	%SiC
1	78.68	79.03	79.09	79.10
2	79.01	79.17	79.12	79.13
3	79.26	79.20	79.20	79.17
4	79.70	79.25	79.23	79.25
Delta	1.02	0.21	0.14	0.14
Rank	1	2	4	3

Table 4. S/N ratio response table for the Surface Roughness

Level	Speed	Feed	DoC	%SiC
1	-6.22	-5.01	-6.46	-4.40
2	-4.95	-5.83	-6.45	-6.51
3	-7.69	-7.76	-5.42	-8.10
4	-7.82	-8.08	-8.36	-7.67
Delta	2.86	3.06	2.94	3.70
Rank	4	2	3	1

Table 5. S/N ratio response table for the Tangential Force

Level	Speed	Feed	DoC	%SiC
1	-37.52	-38.17	-37.72	-39.25
2	-40.09	-40.1	-39.73	-40.51
3	-41.44	-41.92	-41.35	-40.55
4	-43.1	-41.96	-43.35	-41.84
Delta	5.58	3.79	5.63	2.6
Rank	2	3	1	4

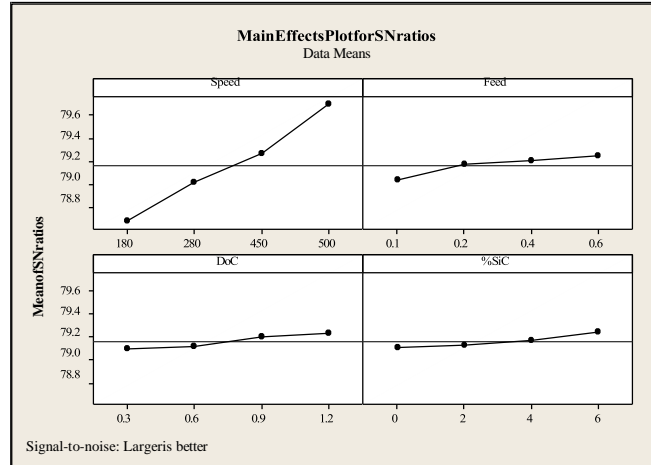


Fig. 4 Mean plot effect for signal-to-noise ratio for material removal rate

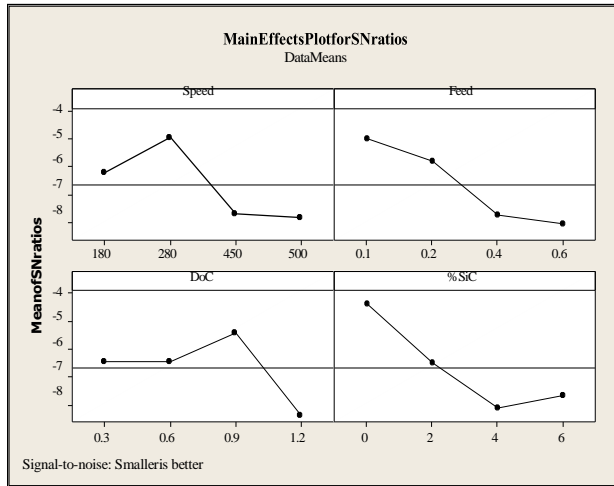


Fig. 5 Mean plot effect for signal-to-noise ratio for Surface Roughness.

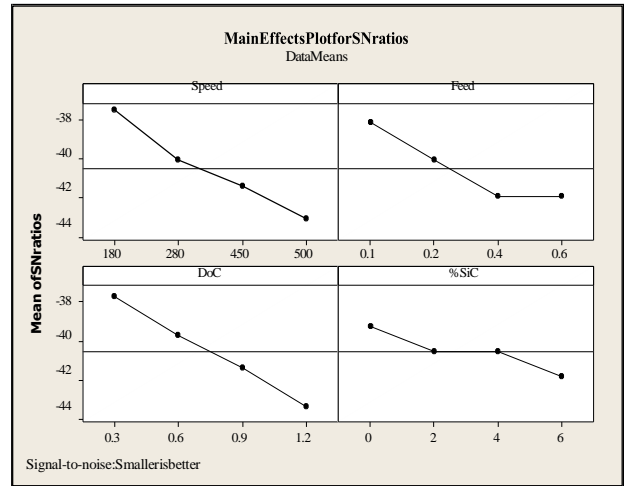


Fig. 6 Mean plot effect for the Noise ratio for Tangential Force

5.5. Analysis of Variance (ANOVA)

ANOVA quantified the relative influence of each factor:

- Cutting speed was the principal contributor to R_a , accounting for approximately 45–50% of the total variance.
- Feed rate was a major driver for MRR (~40% contribution), while DoC significantly affected both MRR and Ft.
- SiC content influenced both R_a and Ft due to the

enhanced hardness and abrasiveness at higher reinforcement levels

- F-tests at the 95% confidence level confirmed the statistical significance of cutting speed and feed rate for machinability responses. Confirmation experiments performed at the predicted optimal settings yielded deviations below 5%, supporting the robustness of the Taguchi-based predictions.

Table 6. ANOVA results for Material Removal Rate

Source	DF	SeqSS	AdjSS	AdjMS	F	P
Speed	3	2.21729	2.21729	0.7391	356.65	0
Feed	3	0.10169	0.10169	0.0339	16.36	0.023
DoC	3	0.04952	0.04952	0.01651	7.97	0.061
%SiC	3	0.04604	0.04604	0.01535	7.41	0.067
Error	3	0.00622	0.00622	0.00207		
Total	15	2.42077				

Table 7. ANOVA results for Surface Roughness

Source	DF	SeqSS	AdjSS	AdjMS	F	P
Speed	3	22.085	22.085	7.362	2.81	0.209
Feed	3	26.592	26.592	8.864	3.39	0.171
DoC	3	18.082	18.082	6.027	2.3	0.255
%SiC	3	32.916	32.916	10.972	4.19	0.135
Error	3	7.847	7.847	2.616		
Total	15	107.522				

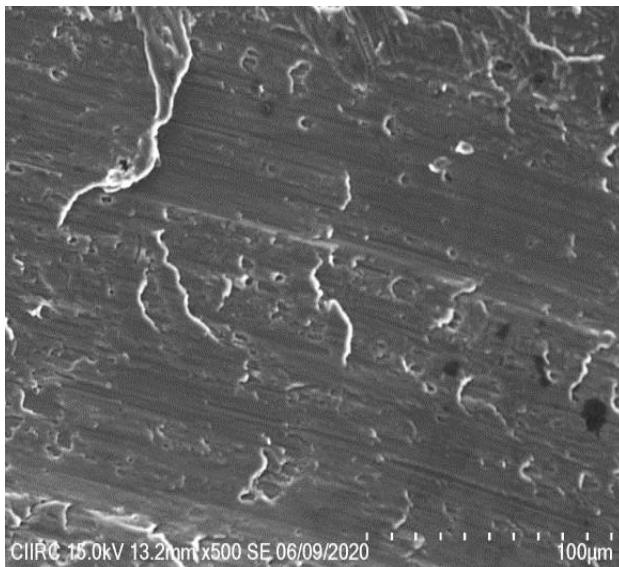
Table 8. ANOVA results for Tangential Force

Source	DF	SeqSS	AdjSS	AdjMS	F	P
Speed	3	66.666	66.666	22.222	40.89	0.006
Feed	3	38.855	38.855	12.952	23.83	0.014
DoC	3	68.599	68.599	22.866	42.08	0.006
%SiC	3	13.503	13.503	4.501	8.28	0.058
Error	3	1.63	1.63	0.543		
Total	15	189.253				

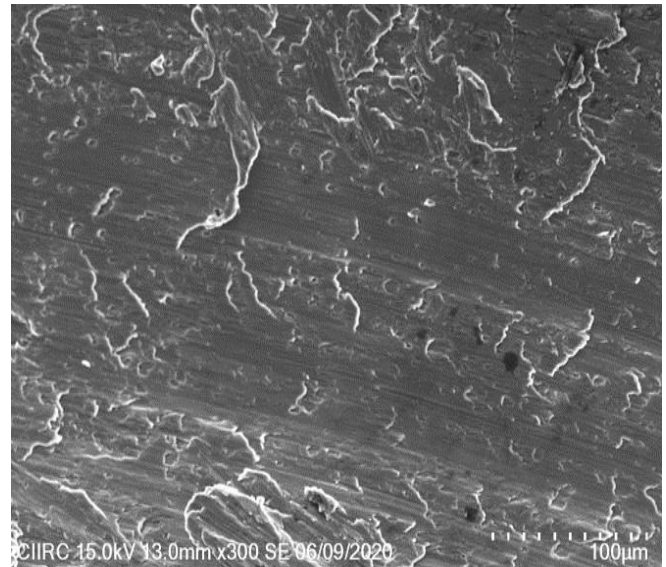
5.6. Chip Formation and Surface Morphology

SEM observations of chips and machined surfaces revealed condition-dependent morphologies. At low cutting speeds, segmented/discontinuous chips were common, consistent with built-up edge formation and insufficient heat evacuation. Increasing cutting speed produced continuous, curled chips with smoother edges, indicative of steadier shear and reduced adhesion.

Machined surfaces exhibited fine grooves and micro-scratches associated with abrasive SiC particulates traversing the cutting zone. Under optimized parameters, surface topography became more uniform with fewer defects, corroborating the improvements predicted by the Taguchi analysis.



(a)



(b)

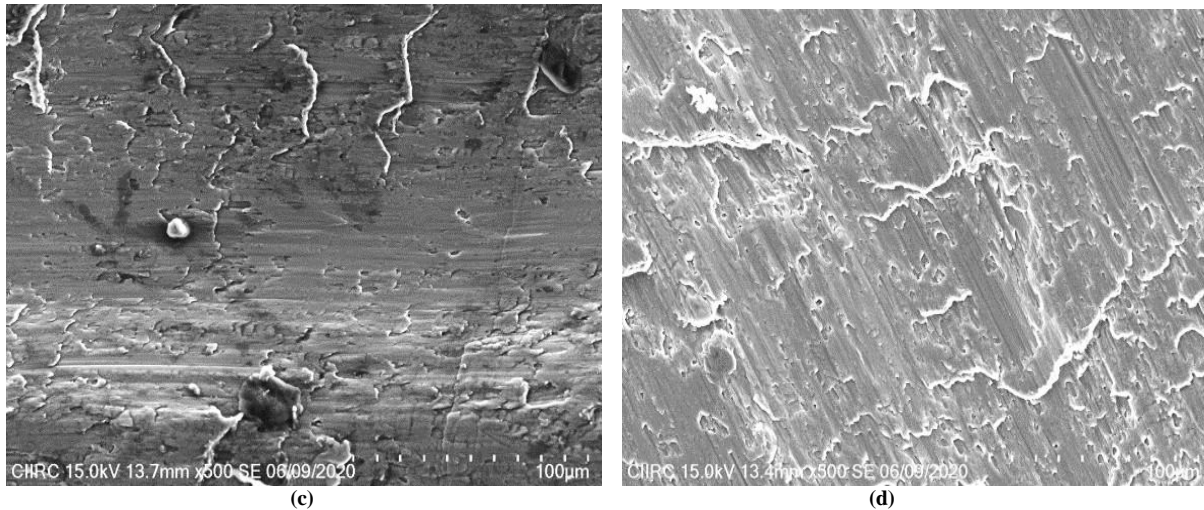


Fig. 7 SEM analysis of the chip formed for (a) 2%, (b) 4%, (c) 6%, and (d) 8%SiC reinforced AA6061 composites at a depth of cut of 0.3 mm, speed 180 rpm, and 0.6 mm/rev.

5.7. Chip Formation Analysis

All SEM micrographs of the chip surface showed lamella structures formed due to periodic tool material surface contact. With 0% SiC content, the Al6061 alloy surface, as seen in the Figure, showed minimal surface roughness with a small number of low-width lamellas. However, with the addition of SiC content, the width and number of lamella structures on the chip were found to increase. With the increase in SiC content from 2% to 8%, the surface roughness of the composite is increasing. This claim is supported by an increase in the width of lamellar chips as seen in Figures 7 (c) and (d). Compared to the Al 6061 alloy, the surface topography of composites was found to have a poor surface finish. Overall, the mechanism responsible for chip formation in the case of composites is ploughing and shearing.

5.8. Summary

- Cutting speed and feed are the primary levers for controlling surface finish and productivity, respectively.
- Increasing SiC content elevates hardness and wear resistance but also raises cutting forces and accelerates tool wear.
- The Taguchi design combined with ANOVA effectively ranks factor influence and predicts optimal conditions with high fidelity.
- Uniform reinforcement dispersion and sound interfaces contribute to consistent machining response.

Overall, the identified turning parameters establish a practical balance between surface quality, throughput, and tool life for Al6061/SiC composites in industrial settings.

6. Future Scope

- Reinforcement design: Vary particle size/shape/distribution; assess hybrids and graded or

dual-scale systems for machinability effects.

- Sustainable cutting: Benchmark dry, flood, MQL/nano-MQL, and cryogenic vs energy use, tool life, and surface integrity.
- Tooling/geometry: Screen PCD/CBN/cermet/coated tools; optimize edge prep, nose radius, and chip-breaker to limit abrasion/adhesion.
- High-speed/thermal: Explore high-speed/high-feed regimes; map temperature via thermocouples/IR and relate to wear and finish.
- Wear and monitoring: Combine post-mortem SEM/EDS with in-situ AE/force/vibration to track wear states and BUE formation.
- Modeling/optimization: Build RSM surfaces; apply multi-objective (NSGA-II) trade-offs; develop ML predictors with Bayesian tuning.
- Physics-based simulation: Calibrate reinforced Johnson–Cook; run FE cutting to predict chip, stress, and temperature; validate experimentally.
- Process generalization: Extend from turning to milling, drilling, and boring; study burrs, hole quality, and tool life for transferable rules.
- Surface integrity/performance: Measure residual stresses, hardness gradients, and subsurface damage; link to tribology, fatigue, and corrosion.
- Processing–machinability links: Compare gravity die with squeeze/ultrasonic/stir processing and T6 heat treatment to relate porosity/interface quality to cutting behavior.
- Reproducibility/data: Include replication, uncertainty, and sensitivity; release open force/AE/surface datasets for benchmarking and model transfer.

7. Conclusion

Al6061/SiC metal matrix composites were produced via the gravity die casting route with a uniform, well-dispersed

reinforcement and clean particle–matrix interfaces. Microstructural evaluations confirmed the absence of reaction layers or interfacial defects, indicating sound bonding and consistent reinforcement distribution across the castings. Process optimization using a Taguchi design, supported by ANOVA, established clear factor–response relationships. Cutting speed emerged as the dominant driver for Material Removal Rate (MRR), SiC fraction exerted the strongest influence on Surface Roughness (Ra), and Depth of Cut (DOC) primarily governed Tangential Cutting Force (Ft). These findings underscore that machinability in Al6061/SiC is controlled by the coupled effects of cutting conditions and reinforcement-induced abrasiveness. SEM assessment of chip morphology revealed surface striations with a lamellar character arising from periodic tool–workpiece interaction. For unreinforced Al6061, chips exhibited narrow, well-ordered lamellae and low roughness, indicative of stable flow. As SiC content increased (2–6 wt%), the lamellae became

wider and more numerous, correlating with higher Ra and stronger abrasive engagement at the tool–chip interface. The prevailing chip formation mechanisms in the composites were ploughing and shearing, initiated by hard SiC particles interrupting the shear front and accelerating tool wear. Overall, judicious selection of cutting speed, feed rate, and DOC can balance surface integrity, cutting forces, and throughput. The results provide a practical, statistically validated basis for setting machining windows that enable reliable and efficient turning of Al6061/SiC components for high-performance engineering applications.

Acknowledgements

The authors express their thanks to the Management of Sanjeevan Engineering & Technology Institute and Principal Sanjeevan Engineering & Technology Institute for their support and encouragement during the research studies.

References

- [1] S. J. Nitesh Kumar et al., “Mechanical Properties of Aluminium-Graphene Composite Synthesized by Powder Metallurgy and Hot Extrusion,” *Transactions of the Indian Institute of Metals*, vol. 70, 605-613, 2017. [[CrossRef](#)] [[Google Scholar](#)] [[Publisher Link](#)]
- [2] Mohan Vanarotti et al., “Surface Modification of SiC Reinforcements & its Effects on Mechanical Properties of Aluminium Based MMC,” *Applied Mechanics and Materials*, vol. 446-447, pp. 93-97, 2014. [[CrossRef](#)] [[Google Scholar](#)] [[Publisher Link](#)]
- [3] Ashwin C. Gowda et al., “Morphology Studies on Mechanically Milled Aluminium Reinforced with B4C and CNTs,” *Silicon*, vol. 11, pp. 1089-1098, 2019. [[CrossRef](#)] [[Google Scholar](#)] [[Publisher Link](#)]
- [4] Avinash Lakshmikanthan et al., “Microstructure, Mechanical and Wear Properties of the A357 Composites Reinforced with Dual Sized SiC Particles,” *Journal of Alloys and Compounds*, vol. 786, pp. 570-580, 2019. [[CrossRef](#)] [[Google Scholar](#)] [[Publisher Link](#)]
- [5] H. Hocheng, *Machining Technology for Composite Materials Principles and Practice*, Woodhead Publishing, 2012. [[Google Scholar](#)] [[Publisher Link](#)]
- [6] Gül Tosun, and Mehtap Muratoglu, “The Drilling of an Al/SiCp Metal-Matrix Composites. Part I: Microstructure,” *Composites Science and Technology*, vol. 64, no. 2, pp. 299-308, 2004. [[CrossRef](#)] [[Google Scholar](#)] [[Publisher Link](#)]
- [7] Gül Tosun, and Mehtap Muratoglu, “The Drilling of Al/SiCp Metal-Matrix Composites. Part II: Workpiece Surface Integrity,” *Composites Science and Technology*, vol. 64, no. 10-11, pp. 1413-1418, 2004. [[CrossRef](#)] [[Google Scholar](#)] [[Publisher Link](#)]
- [8] N.P. Hung et al., “Review on Conventional Machining of Metal Matrix Composites,” *Engineering Systems Design and Analysis*, vol. 75, no. 3, pp. 75-80, 1996. [[Google Scholar](#)]
- [9] S. Singh, “Optimization of Machining Characteristics in Electric Discharge Machining of 6061Al/Al₂O₃p/20P Composites by Grey Relational Analysis,” *The International Journal of Advanced Manufacturing Technology*, vol. 63, pp. 1191-1202, 2012. [[CrossRef](#)] [[Google Scholar](#)] [[Publisher Link](#)]
- [10] S. Ajith Arul Daniel et al., “Multi Objective Prediction and Optimization of Control Parameters in the Milling of Aluminium Hybrid Metal Matrix Composites using ANN and Taguchi -Grey Relational Analysis,” *Defence Technology*, vol. 15, no. 4, pp. 545-556, 2019. [[CrossRef](#)] [[Google Scholar](#)] [[Publisher Link](#)]
- [11] Metin Kök, “Modelling the Effect of Surface Roughness Factors in the Machining of 2024Al/Al₂O₃ Particle Composites based on Orthogonal Arrays,” *The International Journal of Advanced Manufacturing Technology*, vol. 55, pp. 911-920, 2011. [[CrossRef](#)] [[Google Scholar](#)] [[Publisher Link](#)]
- [12] P. Shanmugasundaram, and R. Subramanian, “Influence of Graphite and Machining Parameters on the Surface Roughness of Al-fly Ash/Graphite Hybrid Composite: A Taguchi Approach,” *Journal of Mechanical Science and Technology*, vol. 27, pp. 2445-2455, 2013. [[CrossRef](#)] [[Google Scholar](#)] [[Publisher Link](#)]
- [13] R. Keshavamurthy et al., Effect of Thermo-Mechanical Processing and Heat Treatment on the Tribological Characteristics of Al Based MMC's,” *IOP Conference Series: Materials Science and Engineering: International Conference on Advances in Materials and Manufacturing Applications (IconAMMA-2016)*, Bangalore, India, vol. 149, pp. 1-8, 2016. [[CrossRef](#)] [[Google Scholar](#)] [[Publisher Link](#)]
- [14] Mohan Vanarotti et al., “Study of Mechanical Properties & Residual Stresses on Post Wear Samples of A356-SiC Metal Matrix Composites,” *Procedia Material Science*, vol. 5, pp. 873-882, 2014. [[CrossRef](#)] [[Google Scholar](#)] [[Publisher Link](#)]
- [15] C.S. Ramesh, R. Keshavamurthy, and J. Madhusudhan, “Fatigue Behavior of Ni-P Coated Si₃N₄ Reinforced Al6061 Composites,” *Procedia Materials Science*, vol. 6, pp. 1444-1454, 2014. [[CrossRef](#)] [[Google Scholar](#)] [[Publisher Link](#)]

- [16] G.B. Veeresh Kumar et al., “Studies on Al6061-SiC and Al7075-Al₂O₃ Metal Matrix Composites,” *Journal of Minerals & Materials Characterization & Engineering*, vol. 9, no. 1, pp. 43-55, 2010. [[CrossRef](#)] [[Google Scholar](#)] [[Publisher Link](#)]
- [17] Asif Imran et al., “Tool Wear Parameter Optimization in Machining a Squeeze-Cast Metal Matrix Composite (Al6061-SiC),” *Engineering Proceedings*, vol. 45, no. 1, pp. 1-5, 2023. [[CrossRef](#)] [[Google Scholar](#)] [[Publisher Link](#)]
- [18] S. Sathiyaraj et al., “Optimization of Wear Behaviour of Al6061 Metal Matrix Composites Using Taguchi Approach,” *Turkish Journal of Engineering*, vol. 9, no. 1, pp. 56-63, 2025. [[CrossRef](#)] [[Google Scholar](#)] [[Publisher Link](#)]
- [19] Sagar Kumar Murmu et al., “Exploring Tribological Properties in the Design and Manufacturing of Metal Matrix Composites: An Investigation into the AL6061-SiC-fly ASH Alloy Fabricated via Stir Casting Process,” *Frontiers in Materials*, vol. 11, pp. 1-13, 2024. [[CrossRef](#)] [[Google Scholar](#)] [[Publisher Link](#)]
- [20] D. Elil Raja et al., “Analyzing the Dry Sliding Wear Performance on Aluminum 6061 Alloy Reinforced with SiC And B₄C Hybrid Nanocomposite,” *Advances in Materials Science*, vol. 24, no. 4, pp. 42-56, 2024. [[CrossRef](#)] [[Google Scholar](#)] [[Publisher Link](#)]
- [21] Bhuvanesh Kumar Manickam et al., “Optimization of Drilling Parameters for Al6061/Al6063-SiC-ZrO₂ Composites using TOPSIS Considering Microstructure and Machinability,” *Scientific Reports*, vol. 15, pp. 1-20, 2025. [[CrossRef](#)] [[Google Scholar](#)] [[Publisher Link](#)]
- [22] Gokhan Basar, Funda Kahraman, and Oguzhan Der, “Multi-Response Optimization of Drilling Parameters in Direct Hot-Pressed Al/B₄C/SiC Hybrid Composites Using Taguchi-Based Entropy-CoCoSo Method,” *Materials*, vol. 18, no. 18, pp. 1-33, 2025. [[CrossRef](#)] [[Google Scholar](#)] [[Publisher Link](#)]
- [23] BS. Nithyananda et al., “Machinability Studies on Aluminium-Silicon Carbide-Graphite Hybrid Composites: A Focus on Drilling with HSS Tool,” *Evergreen*, vol. 12, no. 2, pp. 940-951, 2025. [[CrossRef](#)] [[Google Scholar](#)] [[Publisher Link](#)]
- [24] Saurabh Singh, and Sunil Kadiyan, “Analysis of Characterization and Drilling Behaviour of Aluminium Based Hybrid Composites,” *International Journal of Leading Research Publication (IJLRP)*, vol. 6, no. 6, pp. 1-9, 2025. [[CrossRef](#)] [[Google Scholar](#)] [[Publisher Link](#)]